JOURNAL OF MATERIALS SCIENCE 29 (1994) 6413–6419

Size effects due to Cosserat elasticity and surface damage in closed-cell polymethacrylimide foam

W. B. ANDERSON, R. S. LAKES*‡

* University of Wisconsin

This article describes the experimental investigation of Cosserat (or micropolar) elasticity and surface damage effects in closed-cell polymethacrylimide foams of different densities. The method of size effects was used to find the degree of Cosserat behaviour for both cylindrical and square cross-section specimens in bending and torsion. The foams were found to behave as Cosserat materials in which slender specimens appear less stiff than thick ones, provided sufficient care is taken when machining the specimens. Surface damage caused by the machining process may cause the apparent stiffness to decrease with decreasing specimen size, giving an opposite softening size effect.

1. Introduction

Cellular solids are two-phase composite materials in which one phase is solid and the other is a fluid, most often air. If the size scale becomes large enough, the material may no longer be assumed to be continuous. Some researchers have found that classical elasticity theory does not always adequately describe the behaviour of cellular materials. In composite materials with stress concentrations due to holes or cracks, the observed fracture behaviour is not correctly predicted by the classical theory of anisotropic elasticity. The experimental stress concentrations are consistently less than the theoretical ones [1]. The non-classical fracture behaviour has been dealt with using point stress and average stress criteria; however, that approach cannot account for non-classical strain distributions in objects under small load. Strain distributions have been observed in fibrous composites and cellular solids which differ from the predictions of classical elasticity, particularly near small holes and small cracks. Observed concentrations of strain are less than predicted values. Strain fields around large holes, by contrast, follow classical predictions. A more general continuum theory, such as Cosserat elasticity or non-local elasticity, may be of use in predicting non-classical strain distributions.

In this study, size effects in the mechanical rigidity of foams are examined experimentally. Analysis of the results is via generalized continuum mechanics and a model of surface damage.

2. Theories

2.1. Cosserat elasticity

The Cosserat theory of elasticity [2, 3], also called micropolar elasticity [4], incorporates the local rotation of points as well as the translation allowed in classical elasticity. Moreover, there is a torque per unit area, or couple stress, as well as the usual force per unit area, or stress. The rationale is to incorporate some aspects of meso-scale structure of materials in a continuum description of mechanical behaviour. In a foam material viewed as a Cosserat solid, the local rotation can be viewed as the rotation of nodes between ribs in the foam, and the couple stress can be viewed as a spatial average of the bending and twisting moments transmitted by the foam ribs. The constitutive equations for a linear isotropic Cosserat elastic solid are [4]

$$\sigma_{kl} = \lambda\varepsilon_{rr}\delta_{kl} + (2\mu + \kappa)\varepsilon_{kl} + \kappa\varepsilon_{klm}(r_m - \phi_m) \quad (1)$$

$$m_{kl} = \alpha\phi_{r,r}\delta_{kl} + \beta\phi_{k,l} + \gamma\phi_{l,k} \quad (2)$$

in which σ_{kl} is the force stress (which is a symmetric tensor in classical elasticity but is asymmetric here), m_{kl} is the couple stress (or moment per unit area), $\varepsilon_{kl} = (u_{k,l} + u_{l,k})/2$ is the small strain where, u is the displacement, and ε_{klm} is the permutation symbol. The microrotation ϕ_k in Cosserat elasticity is kinematically distinct from the macrorotation $r_k = \varepsilon_{klm}u_{m,l}/2$. The usual Einstein summation convention for repeated indices is used and the comma denotes differentiation with respect to spatial coordinates indicated by the subscripts, which can assume values 1, 2, 3. In three dimensions there are six independent elastic constants required to describe an isotropic Cosserat elastic solid: α, β, γ, κ, λ and μ. The technical engineering constants derived from the elastic constants are presented in Table I [4, 5]. Classical elasticity is a special case, achieved by allowing α, β, γ and κ to become zero. The classical Lamé elastic constants λ and μ then remain and there is no couple stress.

‡ To whom correspondence should be addressed.

0022–2461

TABLE I Cosserat engineering constants

Engineering constant	Formula
Young's modulus	$E = \frac{(2\mu + \kappa)(3\lambda + 2\mu + \kappa)}{2\lambda + 2\mu + \kappa}$
Shear modulus	$G = \frac{2\mu + \kappa}{2}$
Poisson's ratio	$\nu = \frac{\lambda}{2\lambda + 2\mu + \kappa}$
Characteristic length for torsion	$l_t = \left(\frac{\beta + \gamma}{2\mu + \kappa}\right)^{1/2}$
Characteristic length for bending	$l_b = \left(\frac{\gamma}{2(2\mu + \kappa)}\right)^{1/2}$
Coupling number	$N = \left(\frac{\kappa}{2(\mu + \kappa)}\right)^{1/2}$
Polar ratio	$\Psi = \frac{\beta + \gamma}{\alpha + \beta + \gamma}$

For a particular material, the appropriate constitutive equation must be determined by experiment. Cosserat elasticity is thought to offer advantages over classical elasticity in the prediction of stresses in materials with microstructure. In particular, analytical solutions for stress concentrations around circular holes [6] and elliptic holes in plates disclose smaller stress concentration factors in a Cosserat solid as opposed to a classical solid. Similar results have been obtained for the predicted stress intensity factors for cracks in plates as well as planar circular cracks in three-dimensional solids.

Another consequence of Cosserat theory is that a size effect is predicted in the torsion and bending of rods [5]. The apparent modulus of the rods increases as their size decreases. A size-effect behaviour consistent with that predicted by Cosserat theory has been observed in some cellular materials, including bone and some man-made foams [7–9]. The six Cosserat elastic constants were found for some of these materials [7, 9].

2.2. Non-local elasticity

Another generalized continuum theory that has been proposed for the analysis of cellular materials is non-local elasticity. In an isotropic non-local solid the points can only undergo translational motion as in the classical case, but the stress at a point depends not only on the strain at that point, but on the strain in a region near that point. The constitutive equation for an isotropic non-local solid is [10, 11]

$$\sigma_{ij}(x) = \int_V \{\lambda(|x' - x|)\varepsilon_{rr}(x')\delta_{ij} + 2\mu(|x' - x|)\varepsilon_{ij}(x')\}\,dV(x') \quad (3)$$

A simpler representation is

$$\sigma_{ij}(x) = \int_V \{\alpha(|x' - x|)[\lambda\varepsilon_{rr}(x')\delta_{ij} + 2\mu\varepsilon_{ij}(x')]\,dV(x') \quad (4)$$

with the non-local kernel $\alpha(/x/)$ subject to $\int_V \alpha(|x|)dV = 1$, requiring the kernel to be a member of a Dirac delta sequence. So, in the limit of the non-local distance of influence or characteristic length a becoming vanishingly small, the classical Hooke's law is recovered.

As with Cosserat elasticity, there is a size effect predicted in bending and torsion with non-local elasticity. There also is predicted a size effect in tension. However, the size effect in non-local solids may be opposite to that in Cosserat solids, i.e. the apparent elastic moduli would decrease with decreasing specimen size. Lakes [12] showed that this phenomenon arises in bending, torsion and tension when, near the surface, only a portion of the kernel's region of influence is integrated over the stress and hence contributes to it. Thus, if the kernel is positive definite throughout its range, then there is a surface layer of depth a in which the stress is less than the product of Young's modulus E and the strain ε. If the kernel is not positive definite, and goes negative over part of its range, then there may be a stiffening effect of small specimens. So non-local elasticity theory allows both the apparent increase in modulus with decreasing specimen size (as with Cosserat elasticity) and the apparent decrease in modulus with decreasing specimen size.

2.3. The structural view

The physical origins of the size effects predicted in Cosserat elasticity lie in the bending and twisting moments transmitted in the fibres of composites or the ribs in foams. The characteristic length l may be of the order of the spacing between fibres in a composite [13]; in cellular solids it may be related to the average cell size [14]. The characteristic length for macroscopically homogeneous solids such as single crystals or amorphous materials is of the order of the atomic spacing, much too small to be perceptible in any macroscopic mechanical experiment [9].

The physical mechanism underlying non-local elasticity is long-range cohesive force. An example is the electromagnetic force between ions in a crystal. In foams and fibrous systems, the generation of long-range forces is not so easy to visualize.

An alternative to the above continuum views and their associated physical processes is the structural view of edge or surface effects. In a foam, the cells at the edge of a specimen are incomplete. These edge cells contribute to the volume of the specimen, but are not able to carry much load. Hence, the effective stiffness of the specimen is less than would be expected, producing an "anti-Cosserat" effect. Moreover, a surface damage layer would also produce this effect, which becomes more pronounced as the specimen size approaches the cell size. Fig. 1 shows the relative size effects possible due to Cosserat elasticity and an edge-effect model described below, as compared to a classical elastic solid.

The edge-effect model for round specimens is an extension of that developed by Brezny and Green [15] for square specimens. The derivation is described in an

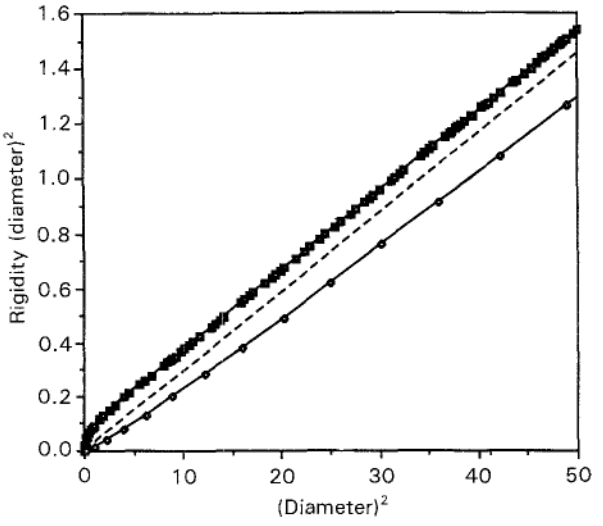

Figure 1 Analytical size-effect curves for rods in torsion under several assumptions: rigidity divided by square of diameter versus square of diameter, assuming $G = 28$ MPa and cell size of 1 mm. Classical elasticity (– – –) gives a straight line through the origin. Cosserat elasticity (■), which incorporates moments carried by cell ribs, gives a stiffening effect of small specimens. Surface damage or incomplete surface cells give a softening effect. The Cosserat curve was derived with $N^2 = 0.49$, $l_t = 0.34$ mm, $\Psi = 1.5$ and $\nu = 0.35$. The edge-effect curve (●) assumes classical material with damage layer thickness $X = 0.5$ cells and modulus ratio $n = 0$.

earlier study [16]. In this method, a beam of diameter d containing an outer layer of thickness X of incomplete or damaged cells can be thought of as a composite, with the inner portion consisting of material 1 with moment of inertia I_1 and modulus E_1 (and G_1), and the outer layer consisting of material 2 with moment of inertia I_2 and modulus E_2 (and G_2). The effect of the damage layer is to reduce the apparent rigidity of small specimens, producing a softening effect with decreased specimen size [15, 16]. The ratio of the apparent modulus (subscript e) to the theoretical modulus (subscript o) is then given by

$$\frac{E_e}{E_o} = \frac{I_e}{I_o} = \frac{1}{d^4}[(d - 2X)^4(1 - n) + nd^4] \quad (5)$$

Where d is the specimen diameter, X the damage layer thickness and n the ratio of the damage layer modulus to the inner material modulus, E_2/E_1. Similar analyses of round and square specimens in torsion yield the same results for relative moment of inertia and relative modulus.

Edge effects of this type have been reported for open-cell carbon foams in bending [15] and were attributed primarily to incomplete cells at the surface. The softening effects were also reported for closed-cell polymethacrylimide foam and open-cell copper foam [16] in both bending and torsion. In this case, edge effects were considered to be caused by both an incomplete cell layer and surface damage due to machining. In the present study a rigid, closed-cell polymethacrylimide foam (Rohacell®, Cyro Industries) was tested in an attempt to reduce the effects of machining damage and discover any Cosserat behaviour. It is hoped that understanding the effects of local inhomogeneities and surface damage will allow substantial improvement in foam mechanical properties and open new applications for cellular materials.

3. Experimental procedure

The Rohacell foam (see above) was tested by the method of size effects [7–9]. Three grades were used: WF51 ($\rho = 0.06\ g\,cm^{-3}$), WF110 ($\rho = 0.11\ g\,cm^{-3}$), and WF300 ($\rho = 0.38\ g\,cm^{-3}$). The cell size of the foams was determined by counting the number of cells along a 10 mm line. Both square and cylindrical cross-section specimens were made. The square cross-section specimens were cut first with a low-speed diamond saw. One specimen from each of three densities was cut. Further reduction in cross-section was accomplished by hand, using abrasive impregnated paper. Very light pressure was used, giving a cutting speed of approximately $0.25\ m\,s^{-1}$. Material was removed at approximately $0.01\ cm^3\,min^{-1}$ for the WF300 foam, $0.02\ cm^3\,min^{-1}$ for WF110 and $0.06\ cm^3\,min^{-1}$ for WF51.

The round specimens were first rough-cut into blocks, then machined round on a lathe. One specimen from each of the three densities of foam was cut, with further reductions in cross-section made with the abrasive method on the lathe. Surface cutting speeds ranging from 0.24 to $0.86\ m\,s^{-1}$ were obtained; material was removed at about $0.007 \pm 0.002\ cm^3\,min^{-1}$ for the WF300 foam; $0.04 \pm 0.01\ cm^3\,min^{-1}$ for WF110 and $0.15 \pm 0.03\ cm^3\,min^{-1}$ for WF51.

The specimens were tested using a micromechanics apparatus described previously [7, 8]. Torque is applied via a permanent magnet attached to the end of a specimen. The magnet is placed at the centre of a Helmholtz coil which produces a uniform magnetic field when an electric current is applied. Angular displacement is measured optically using laser interferometry. The specimens were loaded sequentially in both torsion and bending, and values for rigidity were calculated.

Exact analytical solutions for the torsion and pure bending of a circular cylinder of a Cosserat solid are available. Gauthier and Jahsman [5] developed the solution for a circular cylinder in torsion; for bending the solution was given by Krishna-Reddy and Venkatasubramanian [17]. An approximate solution for a Cosserat rectangular prism in torsion was found by Park and Lakes [18]. This approximation keeps the error under 10% for a wide range of elastic constants, and for $0 \leqslant \beta/\gamma \leqslant 0.6$ [18]. There is also an approximate solution for a square bar in bending. This solution assumes that the ratio β/γ is equal to the negative of the Poisson's ratio and is exact for that case only.

A term to account for surface effects may be included in the analysis for Cosserat elasticity. The rigidity ratios (rigidity of a Cosserat solid over rigidity of a classical solid) for circular cylinders in torsion and bending, respectively, then become

$$\Omega_t = \underbrace{\left[1 + 6\left(\frac{l_t}{a}\right)^2 \left(\frac{1 - (4/3)\Psi\chi}{1 - \Psi\chi}\right)\right]}_{\text{Cosserat}} \underbrace{\left(\frac{(a - X)^4(1 - n)}{a^4} + n\right)}_{\text{Surface effects}} \quad (6)$$

and

$$\Omega_b = \left[1 + 8\left(\frac{l_b}{a}\right)^2 \left(\frac{1-(\beta/\gamma)^2}{1+\nu}\right) + \frac{8N^2[(\beta/\gamma)+\nu]^2}{[\zeta(\delta a)+8N^2(1-\nu)](1+\nu)}\right]$$

Cosserat

$$\times\left(\frac{(a-X)^4(1-n)}{a^4}+n\right) \quad (7)$$

Surface effects

where a is the specimen radius, X the damage zone thickness on the surface of the specimen and n the ratio of the modulus of the damage layer to that of the foam, E_2/E_1. The terms χ and ζ are functions of the Cosserat constants [5, 17]. $\chi = I_1(pa)/pa\ I_0(pa)$, and $p^2 = 2\kappa/(\alpha+\beta+\gamma)$. I_1 and I_0 are the modified Bessel functions of the first kind. $\zeta(\delta a) = (\delta a)^2[(\delta a\ I_0(\delta a) - I_1(\delta a))/(\delta a\ \ I_0(\delta a) - 2I_1(\delta a))]$, and $\delta = N/l_b$. The above formulation assumes a linear superposition of Cosserat stiffening due to rib bending and twisting with the softening effect due to a layer of incomplete cells and/or surface damage. The surface effects term tends to compete with the size effect predicted in Cosserat theory, causing an "anti-Cosserat" effect.

The solutions for the Cosserat solids depend on the elastic constants in complex ways. This makes it difficult to numerically analyse a material based on these equations. The approach used here was to graphically determine the shear and Young's modulus by using a least-squares linear regression of the data on a plot of rigidity divided by the square of the diameter versus the square of the diameter. In classical elasticity, the plot of the data would be expected to pass through the origin. If the Rohacell were a Cosserat elastic material, the plot of the data would be expected to have the same slope, but appear to intercept the vertical axis above zero. If edge effects dominate, however, the plot of the data would appear to intercept the vertical axis below zero. The slopes of the plots are proportional to the elastic shear modulus G for torsion and Young's modulus E for bending, regardless of Cosserat or classical elasticity. The graphically determined moduli were then put into the equations for rigidity, and the other elastic constants could then be varied to find the best fit through the data. The best fit was determined by minimizing the residual error, i.e. the sum of the squares of the deviations with experiment. This is similar to the approach used by Lakes [7].

4. Results and discussion

The results for the square abrasive-machined Rohacell show evidence of Cosserat behaviour for all grades of the foam. In all cases ψ was assumed to be 1.5, since its effect is only seen very near the origin of the graph [5, 17, 18]. Values for G and E were determined from least-squares linear fits of the data. The torsion results of the square cross-section WF300 specimens are shown in Fig. 2; the bending results are in Fig. 3. The dashed lines in the figures represent a classical curve fit. A best-fit Cosserat elastic curve is shown with a solid line. The residual for the classical curve is about 20 times as large as that for the Cosserat curve in both torsion and bending. These curves are typical of the results for the WF110 and WF51 tests; the residual for the classical torsion curve is six times that of the best-fit Cosserat curve for the WF110, and ten times larger for the WF51 data.

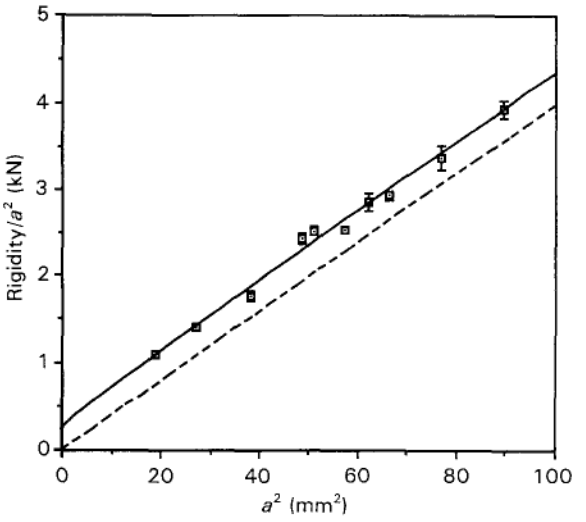

Figure 2 (□) Size-effect results for square, abrasive-machined Rohacell WF300 (width a) in torsion, with Cosserat curve fit for $N^2 = 0.01$. The best-fit curve for this value of N (——) gives $l_t = 0.8$ mm, $l_b = 0.77$ mm and residual error = 3.47 kN^2. The classical curve (– – –) has a residual error of 50.5 kN^2.

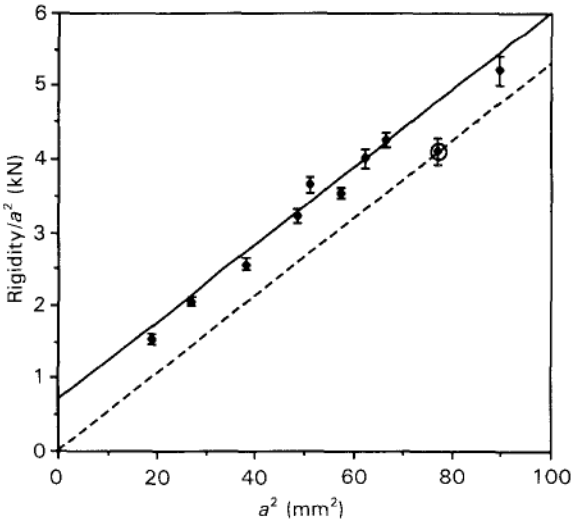

Figure 3 (●) Size-effect results for square, abrasive-machined Rohacell WF300 (width a) in bending. The best-fit Cosserat curve (——) gives $E = 637$ MPa, $l_b = 0.78$ mm, $\nu = 0.13$ and residual error = 34.6 kN^2. The classical curve (– – –) has a residual error of 550 kN^2. One point (circled) is a statistical outlier not used in residual calculations.

The Cosserat engineering constants derived from the best-fit Cosserat curves are given in Table II. Observed cell sizes are also shown in Table II; the error estimate is $\pm$ 0.05 mm. Different trial values for N^2 give similar residuals and characteristic lengths, so the value of N^2 is not well determined. However, there are not enough data points close to the origin to be able to effectively distinguish this curve from the others. More data points at smaller diameters would be needed to determine which curve is most appropriate.

TABLE II Results of size-effect tests on Rohacell foam

Specimen type	Grade	G (MPa)	E (MPa)	N^2	l_t (mm)	l_b (mm)	Cell size (mm)	X/cell size
Square abrasive	WF300	285	637	0.01	0.8	0.77	0.65	–
	WF110	75	216	0.01	0.52	0.35	0.5	–
	WF51	29	66	0.04	0.54	0.55	0.67	–
Round abrasive	WF300[a]	295	–	0.04	0.43	–		–
	WF300[b]	–	672	0.09	0.38	0.48		–
	WF110[a]	75	–	0.01	0.52	0.35		0.08
	WF110[b]	–	215	0.01	0.52	0.35		0.03
	WF51[a]	30	–	0.04	0.54	0.55		0.12
	WF51[b]	–	65	0.04	0.54	0.55		0.20

[a] Torsion tests.
[b] Bending tests.

Of the round specimens machined by the abrasive method, only the WF300 foam demonstrated size effects consistent with Cosserat elasticity. In torsion, the classical curve had a residual only about four times as large as the Cosserat (Fig. 4). There is more scatter in these data than with the square specimens, which may account for the rather large residual error. The curves for the round specimens show an obvious effect of changing the value of N: as N is increased, the curve makes a sharper transition to the linear portion of the curve. This makes it necessary to have data very near the origin (very small specimens) to determine the best value for N. The best-fit bending curve for round WF300 produced a residual factor of eight less than the classical curve (Fig. 5). The square specimens of WF300 produced a residual factor of eight less than values for round specimens. However, the characteristic lengths for the square specimens are nearly twice those of the round specimens. This discrepancy may be due to more surface damage in the round specimens than in the square ones. The rate of material removal with the round specimens was about twice that of the square specimens, possibly leading to more surface machining damage. Such damage would tend to shift the offset of the round specimens toward the classical curve, causing the characteristic lengths to appear smaller than they actually are. Thus, a Cosserat material may appear classically elastic when size effects compete with surface effects such as surface damage and incomplete cells.

Such damage appears to be present in the round specimens of the lower-density WF110 and WF51 grade foams as well. Figs 6 and 7 show the results for the round WF110. In this case the foam appears nearly classical in both bending and torsion. Here, then, the data were analysed with Equations 6 and 7, assuming Cosserat constants as determined with the square specimens, and a damage layer that provided no stiffness, i.e. with modulus ratio $n = 0$. In this manner, a value for the damage layer thickness X could be determined. The results of this analysis are presented in Table II. The damage layer thickness was found to be from about 5 to 20% of the average cell size of the foam. This represents an average thickness; the damage layer at any one point may be thicker or thinner.

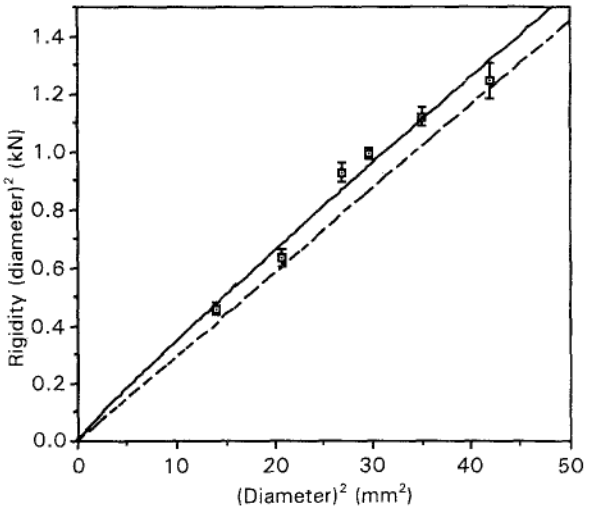

Figure 4 (⊡) Size-effect results for round, abrasive-machined Rohacell WF300 in torsion, with (——) Cosserat curve fit for $N^2 = 0.04$. The best-fit curve for this value of N gives $l_t = 0.43$ mm and residual error = 1.36 kN^2. The classical curve (– – –) has a residual error of 5.83 kN^2.

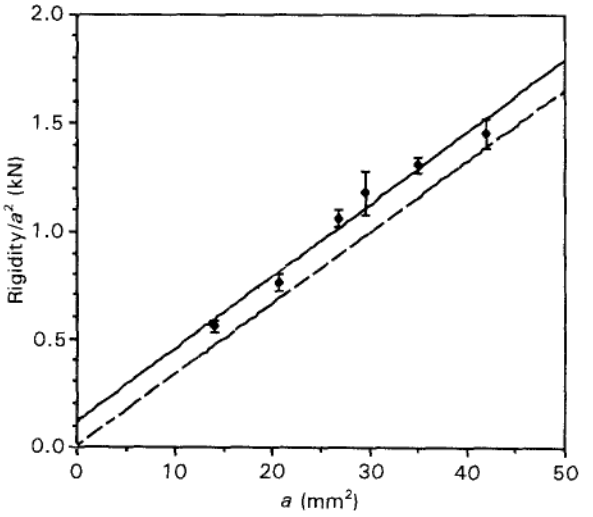

Figure 5 (●) Size-effect results for round, abrasive-machined Rohacell WF300 in bending, with (——) Cosserat curve fit for $N^2 = 0.09$. The best-fit Cosserat curve for this value of N gives $l_t = 0.38$ mm, $l_b = 0.48$ and residual error = 6.89 kN^2. The classical curve (– – –) has a residual error of 48.1 kN^2.

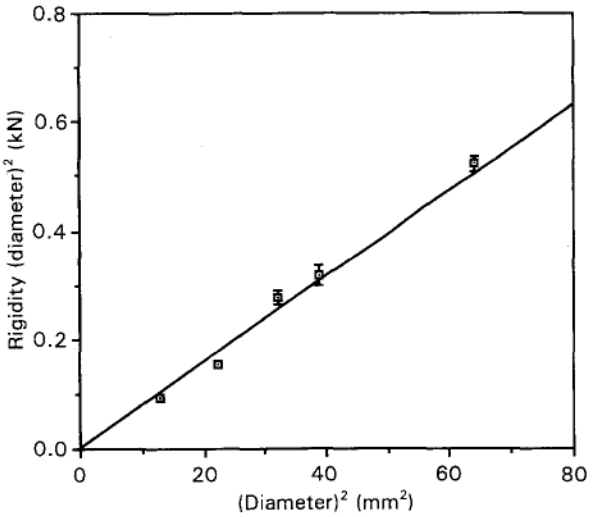

Figure 6 (⊡) Size-effect results for round, abrasive-machined Rohacell WF110 in torsion, with (——) Cosserat curve fit with surface effects for modulus ratio $n = 0$ and damage layer thickness $X = 0.06$ mm (0.1 cells). Cosserat engineering constants used: $N^2 = 0.04$, $l_t = 0.51$ mm, $l_b = 0.36$ mm, $G = 80$ MPa. Residual error = 0.148 kN². The classical curve (not shown) has a residual error of 0.169 kN².

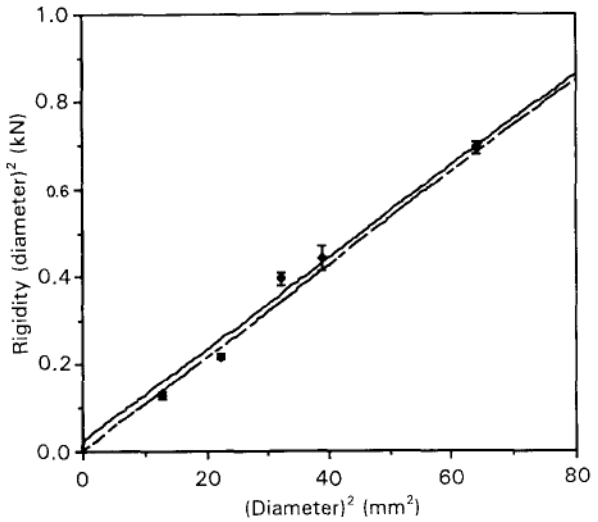

Figure 7 (●) Size-effect results for round, abrasive-machined Rohacell WF110 in bending, with (——) Cosserat curve fit with surface effects for modulus ratio $n = 0$ and damage layer thickness $X = 0.02$ mm (0.04 cells). Cosserat engineering constants used: $N^2 = 0.16$, $l_t = 0.36$ mm, $l_b = 0.49$ mm, $E = 216$ MPa. Residual error = 0.161 kN². The classical curve (– – –) has a residual error of 0.185 kN².

The density of the square specimens remained within 5% of the original density, with no obvious trend. The round specimen density remained within 2% of the original for WF300, 8% of the original for WF110, and 7% of the original for WF51. This suggests that development of a dense surface layer due to subsequent abrasive machining was not responsible for the size effects. Previous experience with copper foam had shown that an increase in material density (in this case caused by plastic compression of the foam during machining) may mimic the size effects predicted by Cosserat elasticity.

The edge effects in the round Rohacell foam appear to be due to machining damage since the square foams demonstrate Cosserat behaviour. Edge effects may also be present in the samples that did show Cosserat behaviour, but the Cosserat effects dominate (which may have caused the discrepancies between the round and square WF300). In fact, at the smallest specimen sizes (about 4 mm) there were only about five to eight cells across an edge. Brezny and Green [15] suggest that at least 15 to 20 cells are necessary to avoid edge effects. The fact that the edge effects appeared in the round specimens and not the square may be attributable to larger volume cutting speeds with the round specimens causing more cell damage at the outer layers.

What the relative effects are of surface damage versus the bending and twisting of ribs in an open or closed-cell foam is unknown. It may be that the surface damage effect is less influential in a closed-cell foam since some of the ribs of the incomplete cells on the surface may be connected by at least a partial face, thereby imparting some stiffness. In the present analysis it was assumed that the damage layer provided zero stiffness in the closed-cell Rohacell. It could also be hypothesized that some non-zero stiffness is provided by the damage layer in closed-cell foams, which would cause the analysis to return a larger value for the damage-layer thickness for the same reduction in specimen rigidity.

One of the important predictions of Cosserat elasticity is the reduction of stress concentration factor for small holes of size approaching the characteristic length. The physical mechanisms underlying Cosserat elasticity may then be viewed as toughening mechanisms. Reduced stress concentration factors for small holes are known experimentally in fibrous composite materials. The fracture strength of graphite epoxy plates with holes depends on the size of the hole [19]. Moreover the strain around small holes and notches in fibrous composites well below the yield point is smaller than expected classically [20, 21], while for large holes the strain field follows classical predictions [22]. Further results are given in the review by Awerbuch and Madhukar [1]. Such results are in harmony with the predictions of generalized continuum mechanics. However, thus far in the fibrous composites community, it has been fashionable to interpret nonclassical results for fracture properties in terms of *ad hoc* criteria rather than to use generalized continua. One such criterion involves attempting to model or predict fracture by calculating the average stress in a region near a stress raiser, rather than using the actual maximum stress. A problem with this approach is that predictive power can be poor if the geometry of the stress concentration is changed. Moreover, point stress criteria do not make any prediction of the stress distribution near stress raisers, so that no prediction of the distribution of microdamage can be obtained.

By contrast, the generalized continuum approach permits the prediction of stress and strain distributions. For example, Cosserat elastic constants obtained via size effects experiments at small strain in human bone (a natural fibrous composite) were used

TABLE III Relation between Cosserat constants and toughness of Rohacell foam (all square specimens, cut by abrasive method)

Grade	ρ (g cm^{-3})	l_t (mm)	l_b (mm)	Cell size (mm)	K_{Ic} (MPa m$^{1/2}$)	$(K_{Ic}/E)^2$ (μm)
WF300	0.38	0.8	0.77	0.65	1.1	15
WF110	0.11	0.52	0.35	0.5	0.19	6.4
WF51	0.06	0.54	0.55	0.67	0.08	7.6

to predict the distribution of strain in a square cross-section bar in torsion. The predicted strain does not tend to zero at the corners of the cross-section, in contrast to the classical prediction. The experimental strain distribution was found to be in good agreement with the predictions of Cosserat elasticity but not with the predictions of classical elasticity [23].

The measured characteristic lengths are associated with the fracture toughness K_{Ic} [24] of Rohacell foam as shown in Table III. l_t correlated well with the normalized toughness $(K_{Ic}/E)^2$, which has the dimensions of length ($r^2 = 0.996$). Toughness correlated well with $\rho^{3/2}$, as anticipated by Gibson and Ashby [25] ($r^2 = 1.000$). However, toughness was not well correlated with cell size, which was about the same for the three densities of foam ($r^2 = 0.09$). This appears to be in disagreement with Gibson and Ashby, who predict that the toughness K_{Ic} is proportional to the square root of cell size; however, we were not able to independently vary cell size in these studies. We remark that these are closed-cell foams, and the structure cannot be assumed independent of density. Cosserat elasticity may be of use in connection with toughness, not only because they are correlated but also because structural features associated with strongly Cosserat elastic behaviour may be intentionally incorporated into materials [26] as a new toughening mechanism.

5. Conclusions

1. Rohacell polymethacrylimide foam behaves as a Cosserat elastic material. Cosserat elastic constants are determined by the method of size effects. The effects are manifested as a stiffening of slender specimens. It is necessary to take great care during cutting to avoid surface damage.

2. Rohacell foam, when it is lathe-cut with no particular care to avoid damage, exhibits a softening size effect which can be modelled by the analysis of Brezny and Green.

3. Cosserat effects are linked with material toughness; however, further study is required to elucidate the connection further.

Acknowledgement

Partial support by the NASA/Boeing ATCAS programme under contract NAS1-18889, and by a University Faculty Scholar Award from the University of Iowa to RL, is gratefully acknowledged.

References

1. J. AWERBUCH and S. MADHUKAR, *J. Reinf. Plast. Compos.* **4** (1985) 3.
2. E. COSSERAT and F. COSSERAT, "Theorie des corps deformables" (Hermann et Fils, Paris, 1909).
3. R. D. MINDLIN, *Int. J. Solids Struct.* **1** (1965) 265.
4. A. C. ERINGEN, in "Fracture" Vol. 1, edited by H. Liebowitz (Academic, New York, 1968) p. 621.
5. R. D. GAUTHIER and W. E. JAHSMAN, *J. Appl. Mech.* **42** (1975) 369.
6. P. N. KALONI and T. ARIMAN, *J. Appl. Math., Phys. (ZAMP)* **18** (1967) 136.
7. R. S. LAKES, *Int. J. Solids Struct.* **22** (1986) 55.
8. *Idem, J. Mater. Sci.* **18** (1983) 2572.
9. *Idem, J. Eng. Mater. Tech.* **113** (1991) 148.
10. E. KRÖNER, *Int. J. Solids Struct.* **3** (1967) 731.
11. A. C. ERINGEN, *Int. J. Engng Sci.* **10** (1972) 425.
12. R. S. LAKES, Boeing Technical Report (Boeing Commercial Airplanes, Seattle, WA, 1993).
13. M. HLAVACEK, *Int. J. Solids Struct.* **112** (1975) 199.
14. G. ADOMEIT, in Proceedings of IUTAM Symposium on Mechanics of Generalized Continua, Freudenstadt, Stuttgart, edited by E. Kroner (Springer, Berlin, 1967).
15. R. BREZNY and D. J. GREEN, *J. Mater. Sci.* **25** (1990) 4571.
16. W. B. ANDERSON, C. P. CHEN and R. S. LAKES, *Cellular Polym.* **13** (1994) 1.
17. G. V. KRISHNA-REDDY and N. K. VENKATASUBRAMANIAN, *J. Appl. Mech.* **45** (1978) 429.
18. H. C. PARK and R. S. LAKES, *Int. J. Solids. Struct.* **23** (1987) 485.
19. R. F. KARLAK, in Proceedings of Conference on Failure Modes in Composites, IV (Metallurgical Society of AIME, Chicago, 1977) p. 106.
20. J. M. WHITNEY and R. J. NUISMER, *J. Compos. Mater.* **8** (1974) 253.
21. I. M. DANIEL, *Exper. Mech.* **18** (1978) 246.
22. R. E. ROWLANDS, I. M. DANIEL and J. B. WHITESIDE, *ibid.* **13** (1973) 31.
23. H. C. PARK and R. S. LAKES, *J. Biomechan.* **19** (1986) 385.
24. S. K. MAITI, M. F. ASHBY and L. J. GIBSON, *Scripta Metall.* **18** (1984) 213.
25. L. J. GIBSON and M. F. ASHBY, "Cellular Solids" (Pergamon, Oxford, UK, 1987) p. 157.
26. R. S. LAKES, *Cellular Polym.* **12** (1993) 17.

Received 8 April
and accepted 10 May 1994